

Strengthening of RC beams with prefabricated RC U cross-sectional plates

Ali Demir*, Muhammed Tekin, Tezcan Turalı and Muhiddin Bağcı

Department of Civil Engineering, Celal Bayar University, Manisa, Turkey

(Received October 7, 2010, Revised January 20, 2014, Accepted February 1, 2014)

Abstract. The topic of this study is to strengthen cracked beams with prefabricated RC U cross-sectional plates. The damaged beams were repaired by epoxy based glue. The repaired beams were strengthened using prefabricated plates. The strengthening plates were bonded to the bottom and side faces of the beams by anchorage rods and epoxy. The strengthened beams were incrementally loaded up to maximum load capacities. The experimental results were satisfactory since the load carrying capacities of damaged beams were increased approximately 76% due to strengthening. It was observed that strengthening plates had a dominant effect on the performance of beams in terms of both the post-elastic strength enhancement and the ductility. The experimental program was supported by a three-dimensional nonlinear finite element analysis. The experimental results were compared with the results obtained from the beam modeled with ANSYS finite element program.

Keywords: prefabricated RC plate; strengthening; load carrying capacity; ductility; epoxy; anchorage rod; ANSYS

1. Introduction

1.1 General

Beams and columns of structures or bridges built long time ago or damaged due to an earthquake or other reasons have to be strengthened. In strengthening of structural elements, increasing the depth of beam and bonding plate methods are frequently used. The techniques used commonly in literature are bonding steel sheets (Swamy *et al.* 1987, Adhikary and Mutsuyoshi 2006, Arslan *et al.* 2008, Su *et al.* 2010, Zhu and Su 2010, Aykac *et al.* 2012) and FRP sheets (Buyukozturk and Karaca 2002, Lu *et al.* 2005, Pham *et al.* 2006, Ceroni 2010, Panda *et al.* 2012, Boukhezar *et al.* 2013). Additionally, structural elements are strengthened by using traditional RC jacketing methods (Altun 2004, Buyukkaragoz 2010, Raval and Dave 2013).

Swamy *et al.* (1987) researched the effect of glued steel plates on the first cracking load, cracking behavior, deformation, serviceability and ultimate strength of RC beams. Altun (2004) determined and compared experimentally the mechanical properties of R/C beams under simple bending, before and after jacketing by R/C again. It was noted that the mechanical behaviors of the

*Corresponding author, Assistant Professor, E-mail: ali.demir@cbu.edu.tr

jacketed R/C beams were similar to and slightly better than those ordinary R/C beams of the same dimensions, despite the fact that the core parts of the jacketed R/C beams were in a yielded state. Adhikary and Mutsuyoshi (2006) presented the results of a parametric study accounting for the effects on beam behavior of plate depth/beam depth ratio, plate thickness, concrete strength and internal shear reinforcement ratio. The effects of each parameter on shear strength of beams with web-bonded steel plates were discussed. Ceroni (2010) presented the results of an experimental program of RC beams equipped of external strengthening made of carbon FRP sheets or Near Surface Mounted FRP carbon bars. The end or distributed U-shaped anchoring devices were applied when the strengthening was made of FRP carbon sheets. Comparisons between experimental and theoretical failure loads were discussed. Aykac *et al.* (2012) investigated the influence of the use of perforated steel plates instead of solid steel plates on the ductility of RC beams. The beams strengthened with various bonding techniques were subjected to monotonic loading. As a result of tests, ductility and energy absorption capacity of beams were significantly increased but it was observed that thickness of plate had little effect on the bending rigidity of the beam. Panda *et al.* (2012) conducted an experimental investigation on the performance of RC T-beams strengthened in shear using epoxy bonded glass fiber fabric. The effectiveness, the cracking pattern and modes of failure of strengthened beams were evaluated. The load carrying capacity of beams strengthened in shear with U-jacketed GFRP sheets increased by 10-46%.

In this study, the damaged beams were strengthened by prefabricated RC plates instead of traditional jacketing. The strengthening plates having U cross-section were bonded to the three faces of the beams by epoxy and anchorage rods. The strengthened beams were incrementally loaded up to maximum load capacities. The results of the experiments were compared with the results obtained from the beam modeled with ANSYS nonlinear finite element program. It is observed that the strengthening method proposed can be useful, practical and reliable for a structure or a bridge having similar beams.

1.2 Advantages and disadvantages of the proposed method

Some methods used in practice have shortcomings such as fire, corrosion, debonding under loading and making so much effort. Contrary to these, fire and corrosion problems are not in question for this technique which is easily applicable, economic and sufficient with regard to capacity increasing. However, the mould, reinforcement and concrete workmanships in situ don't require in comparison with traditional jacketing. Since the strengthening plate is made of the same material as the beams, it is thought that this method may be more aesthetic. But the proposed technique increases dead weight of structures. Although it is a disadvantage for both this technique and all of jacketing methods, this problem can be minimized using thin plates and lightweight concrete.

2. Experimental program

2.1 Test setup

All beams were incrementally loaded up to maximum load capacities in order to define the load-displacement relationship. A single point bending test setup was adopted, as shown in Fig. 1. The beams were simply supported with the clear distance of 1800 mm between the supports and



Fig. 1 Un-strengthened RC beam

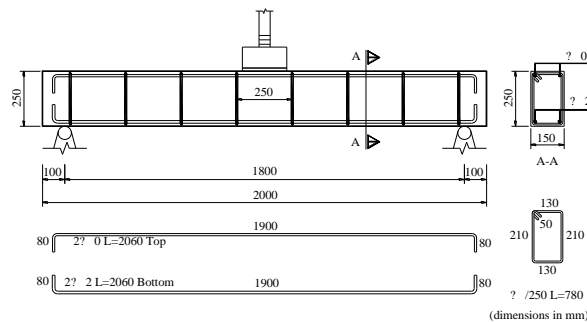


Fig. 2 Detail of Un-strengthened RC beam

loaded at mid-span. Load was applied by a 250 kN hydraulic jack in the vertical direction. Mid-span displacement of beams was measured with the help of a linear variable displacement transducer (LVDT). The beam was incrementally loaded up to the failure. For each increment of the load, the displacements were measured by the help of LVDTs placed at mid-span.

2.2 Specimen details

The existing beam size used was 150 mm (b) \times 250 mm (h) \times 2000 mm (l). Stirrups of 8 mm in diameter and 250 mm in interval were applied throughout the span of the beam. The existing beams named as “B1, B2, B3” were reinforced with two $\text{Ø}10$ bars (10 mm in diameter) in the compression zone, two $\text{Ø}12$ bars (12 mm in diameter) in the tension zone, as shown in Figs. 1-2.

The U cross-sectional prefabricated RC strengthening plates named as “c1, c2, c3” were as shown in Fig. 3. The strengthening plates had been produced before they were bonded to the beams. The plates with 80 mm in thickness were reinforced with two $\text{Ø}12$ bars (12 mm in diameter) in the compression and tension zones. Stirrups of 8 mm in diameter and 150 mm in interval were applied as seen in Fig. 3.

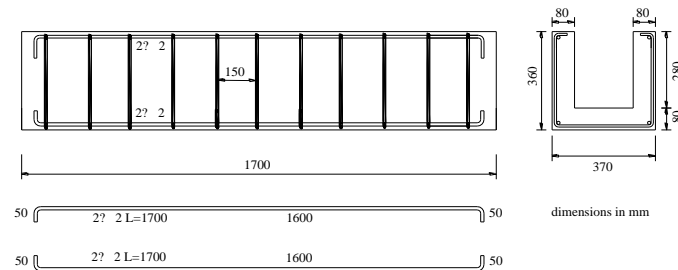


Fig. 3 Prefabricated U cross-sectional RC strengthening plate

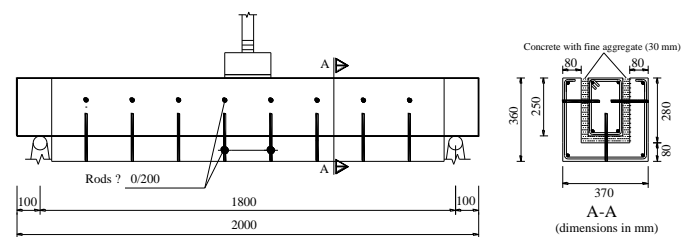


Fig. 4 Detail of RC beam strengthened with prefabricated U cross-sectional RC plate

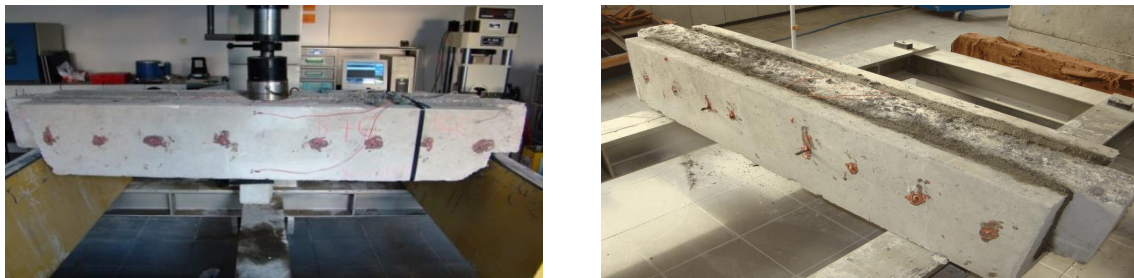


Fig. 5 RC beam strengthened with prefabricated U cross-sectional RC plate

2.3 Bonding procedure

The strengthening plates were bonded to the bottom and side faces of the repaired beams by epoxy and anchorage rods as seen in Figs. 4-5. Before the anchorage rods of 10 mm in diameter were applied, the holes of 12 mm in diameter on the three faces of the beams and strengthening plates were opened. These holes were filled by epoxy and the anchorage rods were driven about 150 mm into the holes.

The cross-section and reinforcement properties of the un-strengthened and strengthened beams, technical properties of epoxy were detailed in Tables 1-2, respectively.

2.4 Material properties

A concrete mix containing maximum coarse aggregates of 10 mm was prepared. The cube strength of specimens was designed for 16 MPa at 28 days. The constituents and the corresponding proportions of the concrete mix were detailed in Table 3.

Table 1 Properties of elements

Specimen	Tension Bars	Stirrups (mm)	Depth (mm)	Width (mm)
B (Un-strengthened beams)	2Ø 12	Ø 8/250	250	150
c (Strengthening plates)	2Ø 12	Ø 8/150	360	370
B-c (Strengthened beams)	4Ø 12	-	360	370

Table 2 Technical properties of epoxy

Bond Strength ASTM C882-91 ¹	12,4 MPa (7 day cure)
Compressive Strength ASTM D-695-96 ¹	82,7 MPa
Compressive Modules ASTM D-695-96 ¹	1493 MPa
Tensile Strength 7 day ASTM D-638-97	43,5 MPa
Base Materials	Concrete
Anchor Type	Chemical Anchor
Material Composition	Epoxy-adhesive
Base Material Temperature-range	-5°C-40°C

Table 3 Concrete mix adopted for producing a cubic meter of concrete

	Water/Cement	Water	Cement	Fine aggregate	10 mm aggregate
kg/m ³	0,6	180	300	960	960

Table 4 Test results of cube specimens

Specimen	Specimen Dimensions (mm)	Axial Load (kN)	Compressive Strength (MPa)
B1	150×150×150	385,9	17,15
c1	150×150×150	411,8	18,05
B2	150×150×150	362,9	16,13
c2	150×150×150	354,8	15,77
B3	150×150×150	397,1	17,65
c3	150×150×150	443,0	19,69

Table 5 Properties of reinforcements

Bar size (mm)	Modulus of elasticity, E_s (MPa)	Yield Strength (MPa)	Ultimate Strength (MPa)
8	210000	430	670
10	210000	425	660
12	210000	427	665

For each specimen, three concrete cubes with dimensions 150 mm × 150 mm × 150 mm were cast and compressive tests were carried out on the test day to obtain the compressive strength of cubes. The average compressive strength of cubes was as shown in the Table 4.

Three samples were taken from each type of reinforcement. The tensile tests were carried out and the yield strength and modulus of elasticity of these samples are summarized in Table 5.

3. Finite element method

In order to support the experimental results, a nonlinear finite element model with ANSYS (2007) was used to determine the ultimate load capacity of the beams. The properties and geometric characteristics of the beam in the nonlinear finite element model were the same as in the tested beams. Material properties of concrete and steel reinforcement in nonlinear finite element analysis were below.

3.1 Concrete

In this study, Hognestad concrete model was used due to lack of confinement for the concrete (Hognestad 1951). The stress-strain values obtained from this model were used in the definition of the multilinear isotropic model. Additionally, the Willam-Warnke failure model (Willam and Warnke 1974) used in the definition of the concrete. In the Hognestad concrete model, the part of stress strain curve until to the peak considered being parabolic in the second degree; and the downward part considered to be linear as seen in Fig. 6. In the model, the formula for the parabola of the curve until the peak is given in Eq. (1) and for the maximum deformation in Eq. (2).

$$\sigma_c = f'_c \left[\frac{2\varepsilon_c}{\varepsilon_{co}} - \left(\frac{\varepsilon_c}{\varepsilon_{co}} \right)^2 \right] \quad (1)$$

$$\varepsilon_{co} = \frac{2f'_c}{E_c} \quad (2)$$

where f'_c is the ultimate compressive strength; σ_c the compressive strength at i^{th} point; ε_{co} the strain at the ultimate compressive strength f'_c ; ε_c the strain at the σ_c compressive strength; E_c is the modulus of elasticity of the concrete.

According to the multilinear isotropic model suggested by Von Mises, the behavior of the concrete in the principle stressing space with three axes is defined in Eq. (3).

$$\sigma_y \geq \sigma_e = \left[\frac{1}{2} \left[(\sigma_1 - \sigma_2)^2 + (\sigma_2 - \sigma_3)^2 + (\sigma_3 - \sigma_1)^2 \right] \right]^{\frac{1}{2}} \quad (3)$$

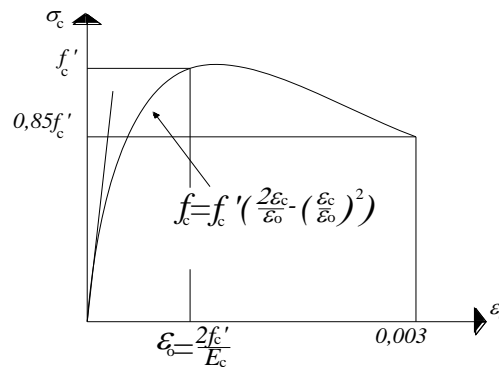


Fig. 6 Hognestad's concrete model

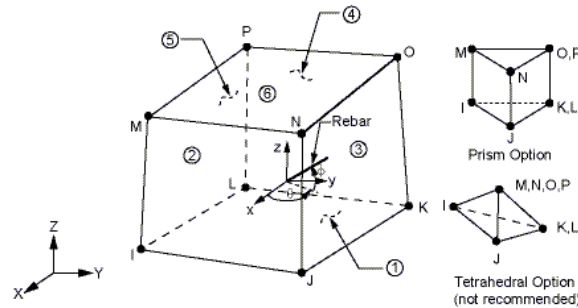


Fig. 7 Solid65 element

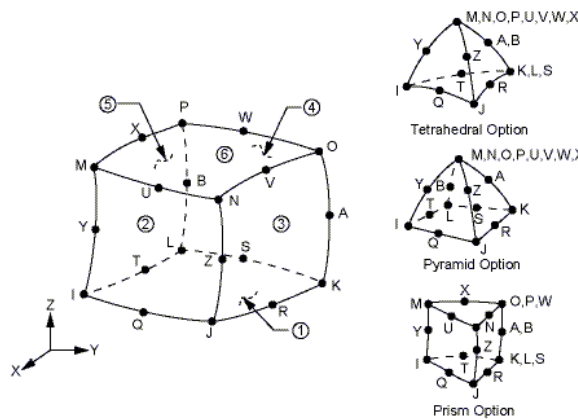


Fig. 8 Solid95 element

where σ_y is the threshold stress in passing from elastic to plastic behavior; σ_c is the equivalent stress less than threshold stress and σ_1, σ_2 and σ_3 are principal stresses.

The Willam-Warnke failure model is used for modeling the failed collapsing surface of concrete without reinforcement under stress with three axes. If the calculated principle stress is more than the threshold stress, its behavior is considered to be nonlinear. In this case, the calculated principle stresses are used to determine the failure situation using the Willam-Warnke model. If Eq. (4) is obtained using these principals, it means that stresses occur on the failure surface.

$$\frac{1}{\rho} \frac{\sigma_a}{f_c} + \frac{1}{r(\theta)} \frac{\tau_a}{f_c} = 1 \tag{4}$$

where σ_a and τ_a are average stress components, z is the apex of the surface and f_c is the uni-axial compressive strength, r is the position vector locating the failure surface with angle θ .

Solid65 is used for the 3-D modeling of solids with or without reinforcing rebars as shown in Fig. 7. The solid is capable of cracking in tension and crushing in compression (ANSYS 2007).

3.2 Steel reinforcement

The steel is a homogeneous and isotropic material which can be defined more easily and closer

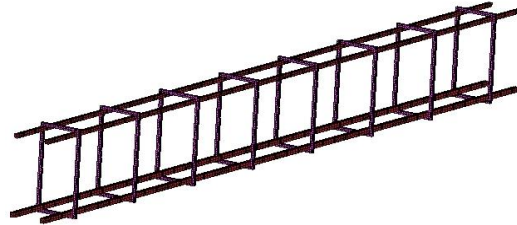


Fig. 9 Reinforcement and stirrup model of B1

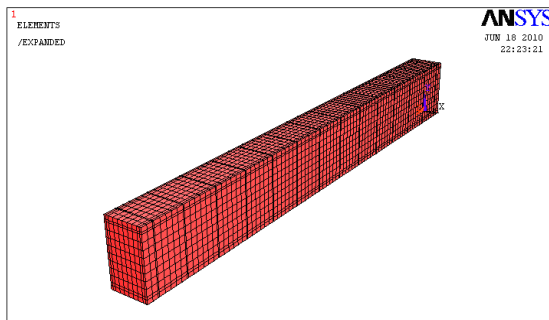


Fig. 10 Finite element model of B1

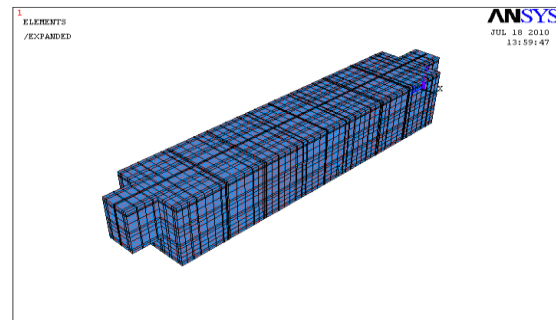


Fig. 11 Finite element model of B1c1

to reality than concrete. Unlike concrete, its properties do not depend on environmental conditions and time. Solid95 element is used in order to define the reinforcement that present in ANSYS finite element program (ANSYS 2007) as seen in Fig. 8.

In this study, discrete modeling was used for reinforcement and stirrup steel in finite element analyses as seen in Fig. 9.

A three-dimensional nonlinear finite element model and the typical finite element meshes of the un-strengthened beam B1, strengthened beam B1c1 were shown in Figs. 10-11.

4. Experimental and finite element results

The experimental and finite element results were presented and discussed in terms of the ultimate load, displacement, ductility and mode of failure.

4.1 Experimental strength and ductility

The beams B1, B2, B3 were loaded until flexural cracks started to occur. These cracks were repaired with epoxy and the strengthening plates were bonded to the beams. The strengthened beams were then loaded up to maximum capacity. The strengthened beams showed various percentage of strengthening ranging from 74% to 78%. The experimental failure loads and increase in load carrying capacities were tabulated in Table 6.

The experimental load-displacement curves of the beams are shown in Fig. 12 and idealized by a bi-linear curve as shown in Fig. 13. The displacement ductility factor μ , which is defined as the ratio between the displacement at peak load Δ_u and the notional yield displacement Δ_y is adopted

Table 6 Experimental failure loads and capacity increases for beams

Specimen	B1	B1c1	B2	B2c2	B3	B3c3
Experimental Failure Loads (kN)	45,30	80,10	43,10	76,59	48,10	83,88
Increase in Load Capacity due to Strengthening %		77		78		74

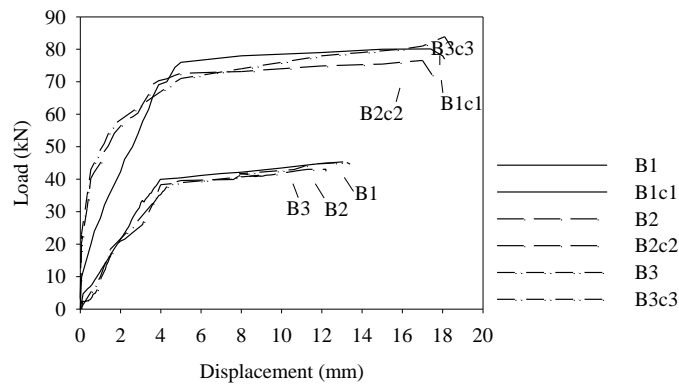


Fig. 12 Experimental load–mid-span displacement curves for un-strengthened and strengthened beams

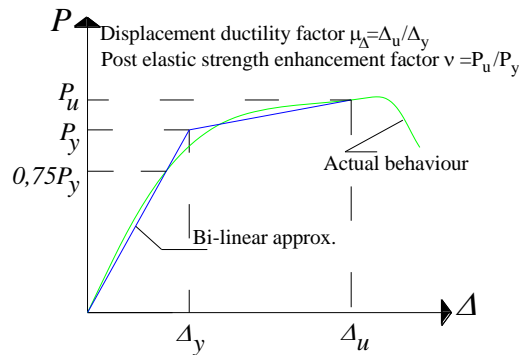


Fig. 13 Definitions of displacement ductility factor and post-elastic strength enhancement factor

to measure the ductility performance of the strengthened beams (Su *et al.* 2010). The displacement ductility factors of all beams were calculated using the above definitions and the results were tabulated in Table 7. The all beams have displacement ductility, ranging from 3,00 to 4,07. The displacement ductility of un-strengthened beams was lower than the strengthened beams as expected.

Substantial post-elastic strength enhancement can be found as shown in Fig. 12. The post-elastic strength enhancement factor v is defined as the ratio between the peak strength P_u and the yield strength P_y , see Fig. 13 (Su *et al.* 2010). The post-elastic strength enhancement factors of the beams were tabulated in Table 7. The all beams have post-elastic strength enhancement factor, ranging from 1,06 to 1,24.

Table 7 Comparison of displacement ductility factors and post-elastic strength enhancement factors

Specimen	Δ_y (mm)	Δ_u (mm)	μ	P_y (kN)	P_u (kN)	ν
B1	3,98	13,06	3,28	40,54	45,30	1,12
B1c1	5,11	17,40	3,41	75,88	80,10	1,06
B2	4,06	12,20	3,00	36,82	43,10	1,17
B2c2	4,18	17,00	4,07	70,57	76,59	1,09
B3	4,16	13,20	3,17	38,71	48,10	1,24
B3c3	4,50	18,10	4,02	70,01	83,88	1,20

μ =displacement ductility, ν = the post-elastic strength enhancement factor



Fig. 14 Failure of strengthened beam

4.2 Failure modes

Although all of the un-strengthened beams failed in bending, with vertical cracks, the strengthened beams failed by concrete cracking. The failure of strengthened beams was associated with concrete cracks prior to yielding of the reinforcement in the beam. Load carrying capacities of the beams strengthened with the U plates were considerably enhanced. Although the strengthening plates were not significantly damaged during experiments, original beam in U plate reached load carrying capacity. When the strengthened beams failed, capacity of the anchorage rods had not been reached. Experimental failure processes of B1c1, B2c2 and B3c3 were similar.

4.3 Finite element analysis results

Numerical failure loads and load-displacement relationships were compared with the experimental results. Comparison of experimental and ANSYS results were given in Table 8. It was observed that the B1 reached capacity at 45,30 kN load level and B1c1 failed at 80,10 kN at the end of experimental loading. The load carrying capacity of B1c1 increased 77% in test. In the finite element analyses, pointed load was applied at negative direction of y-axis as seen in Fig. 10. It was observed that the B1 failed at 45,60 kN load level and B1c1 failed at 81,00 kN load at the end of finite element analyses. The load carrying capacity of B1c1 increased 78% in analysis.

The comparison of experimental and ANSYS load-mid-span displacement curves for un-strengthened and strengthened beams were shown in Fig.15. Experimental and ANSYS damages of B1 and B1c1 were shown in Figs.16-17, respectively.

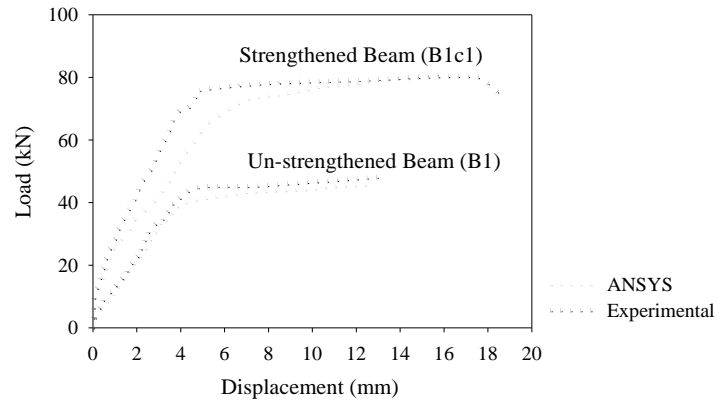


Fig. 15 Comparison of experimental and ANSYS load–mid-span displacement curves for un-strengthened and strengthened beams

Table 8 Comparison for experimental and ANSYS results of un-strengthened and strengthened beams

Specimen	Experimental		ANSYS		Load Capacity Diff. %
	Load Capacity (kN)	Displacement (mm)	Load Capacity (kN)	Displacement (mm)	
B1	45,30	13,06	45,60	12,61	0,66
B1c1	80,10	17,40	81,00	15,90	1,12

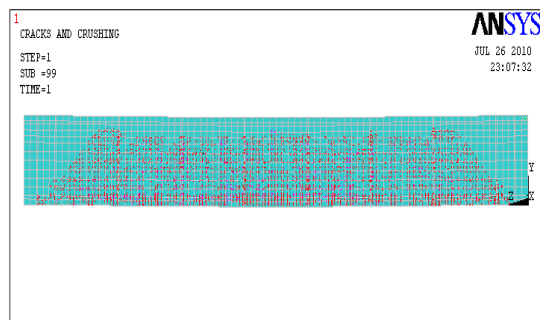


Fig. 16 Cracks of B1 beam at failure

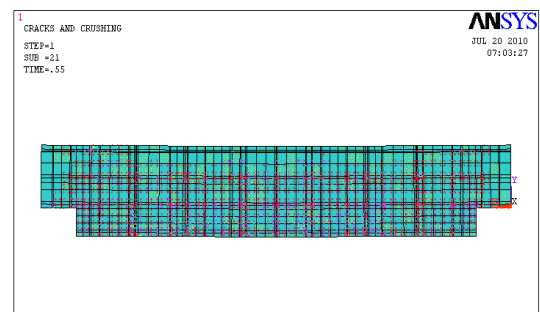


Fig. 17 Cracks of B1c1 beam at failure

5. Conclusions

A new strengthening method for RC beams is proposed in this study. The strengthening method proposed can be a good alternative to strengthening with FRP sheet and steel plates bonding or traditional jacketing. It is thought that lateral load carrying capacity increases since the dimensions of the beams enlarge. Additionally, the moment and shear capacities of beams are increased. Since the strengthening plate is made of the same material as the beams, it is more aesthetic and economic.

The post-elastic strength enhancement and displacement ductility are identified as two important structural performance criteria for structures predominantly subjected to gravity loads. It was seen that these two criteria were greatly influenced by the prefabricated strengthening plates. It was observed that sufficient ductility and strength enhancement could be achieved by the strengthening plates. The load carrying capacities of damaged beams were enhanced approximately 76% with strengthening plates.

The experimental and ANSYS load–displacement curves for un-strengthened and strengthened beams were compared. It was seen that the experimental cracking loads obtained for the beams were close to the results obtained by ANSYS.

Depending on the reasons mentioned above it can be said that the strengthening method investigated both experimentally and numerically is practical, reliable and economic. More experimental and theoretical studies are recommended for the better determination behavior of beams strengthened with prefabricated RC plates.

Acknowledgements

The research described in this paper was financially supported by the Scientific Research Project Commission of Celal Bayar University (Project No. Muh2007-22 and Muh2010-41) and ER PREFABRIK Corporation.

References

- Adhikary, B.B. and Mutsuyoshi, H. (2006), “Shear strengthening of RC beams with web-bonded continuous steel plates”, *Constr. Build. Mater.*, **20**, 296-307.
- Altun, F. (2004), “An experimental study of the jacketed reinforced-concrete beams under bending”, *Constr. Build. Mater.*, **18**, 611-618.
- ANSYS (2007), “Finite element computer program. Version 11”, ANSYS, Inc, Canonsburg (PA).
- Arslan, G., Sevuk, F. and Ekiz, I. (2008), “Steel plate contribution to load-carrying capacity of retrofitted RC beams”, *Constr. Build. Mater.*, **22**, 143-153.
- Aykac, S., Kalkan, I. and Uysal, A. (2012), “Strengthening of reinforced concrete beams with epoxy-bonded perforated steel plates”, *Struct. Eng. Mech.*, **44**(6), 735-751.
- Boukhezar, M., Samai, M.L., Mesbah, H.A. and Houari, H. (2013), “Flexural behaviour of reinforced low-strength concrete beams strengthened with CFRP plates”, *Struct. Eng. Mech.*, **47**(6), 819-838.
- Buyukkaragoz, A. (2010), “Finite element analysis of the beam strengthened with prefabricated reinforced concrete plate”, *Sci. Res. Essays*, **5**(6), 533-544.
- Buyukozturk, O. and Karaca, E. (2002), “Characterization and modeling of debonding in RC beams strengthened with FRP composites”, *Proceedings of 15.ASCE Engineering Mechanics Conference*,

- Columbia University, New York, June.
- Ceroni, F. (2010), "Experimental performances of RC beams strengthened with FRP materials", *Constr. Build. Mater.*, **24**, 1547-1559.
- Hognestad, E. (1951), "A study of combined bending and axial load in RC members", *Univ. Illinois Eng. Exp. Stat. Bull.*, **399**(2), 36-57.
- Lu, X.Z., Teng, J.G., Ye, L.P. and Jiang, J.J. (2005) "Bond-slip models for FRP sheets/plates bonded to concrete", *Eng. Struct.*, **27**(6), 920-937.
- Panda, K.C., Bhattacharyya, S.K. and Barai, S.V. (2012), "Shear behaviour of RC T-beams strengthened with U-wrapped GFRP sheet", *Steel Compos. Struct.*, **12**(2), 149-166.
- Pham, H., Al-Mahaidi, R. and Sauma, V. (2006), "Modeling of CFRP concrete bond using smeared and discrete cracks", *Compos. Struct.*, **75**, 145-150.
- Raval, S.S. and Dave, U.V. (2013), "Effectiveness of various methods of jacketing for RC beams", *Procedia Engineering*, **51**, 230-239.
- Su, R.K.L., Siu, W.H. and Smith, S.T. (2010), "Effects of bolt plate arrangements on steel plate strengthened reinforced concrete beams", *Eng. Struct.*, **32**, 1769-1778.
- Swamy, R.N., Jones, R. and Bloxham, J.W. (1987), "Structural behaviour of reinforced concrete beams strengthened by epoxy-bonded steel plates", *Struct. Eng.*, **65**(2), 59-68.
- Willam, K.J. and Warnke, E.P. (1974), "Constitutive model for triaxial behavior of concrete", *Proceedings of the International Association of Bridge and Structural Engineering Conference*, 174-191.
- Zhu, Y. and Su, R.K.L. (2010), "Behavior of strengthened reinforced concrete coupling beams by bolted steel plates, Part 2: evaluation of theoretical strength", *Struct. Eng. Mech.*, **34**(5), 563-580.